

A Hybrid Quantum-Classical Hamiltonian Learning Algorithm

Youle Wang,^{1,2} Guangxi Li,^{1,2} and Xin Wang²

¹Center for Quantum Software and Information,
University of Technology Sydney, NSW 2007, Australia

²Institute for Quantum Computing, Baidu Research, Beijing 100193, China

Hamiltonian learning is crucial to the certification of quantum devices and quantum simulators. In this paper, we propose a hybrid quantum-classical Hamiltonian learning algorithm to find the coefficients of the Pauli operator components of the Hamiltonian. Its main subroutine is the practical log-partition function estimation algorithm, which is based on the minimization of the free energy of the system. Concretely, we devise a stochastic variational quantum eigensolver (SVQE) to diagonalize the Hamiltonians and then exploit the obtained eigenvalues to compute the free energy's global minimum using convex optimization. Our approach not only avoids the challenge of estimating von Neumann entropy in free energy minimization, but also reduces the quantum resources via importance sampling in Hamiltonian diagonalization, facilitating the implementation of our method on near-term quantum devices. Finally, we demonstrate our approach's validity by conducting numerical experiments with Hamiltonians of interest in quantum many-body physics.

I. INTRODUCTION

The verification of Hamiltonian is an essential direction in certifying the quantum devices and simulators. One general approach for this purpose is the Hamiltonian learning task, which is supposed to recover the Hamiltonian from measurements performed on the system. Recovering large-scaled Hamiltonians expands beyond the power of conventional computers [1, 2]. Thus it is desirable to have an efficient method that takes advantage of quantum computers to reduce the computational resources [3, 4]. While the methods using quantum computers are likely to require the fault-tolerant quantum computers, which are not within reach in the near-term noisy intermediate-scaled quantum (NISQ) era [5]. Hence, it is highly desirable to develop an effective Hamiltonian learning method implementable on NISQ computers.

Various proposed frameworks for Hamiltonian learning are based on the system's dynamics [6–8] or Gibbs states [9–11]. Some frameworks based on dynamics characterize the Hamiltonian by performing quantum simulations that are classically intractable [12] and difficult to implement on near-term quantum computers. To avoid these issues, we adopt a strategy based on Gibbs states, proposed in Ref. [13]. This strategy transforms the Hamiltonian learning task into an optimization program with a suggested solution. Following, we briefly review this strategy.

Consider an n -qubit many-body system's Hamiltonian with a decomposition in Pauli bases as $H = \sum_{\ell=1}^m \mu_{\ell} E_{\ell}$ where each decomposition coefficient $\mu_{\ell} \in [-1, 1]$, each Pauli basis $E_{\ell} \in \{X, Y, Z, I\}^{\otimes n}$ and m denotes the total number of items which scales of $O(\text{poly}(n))$. In the setting, one cannot access the Hamiltonian directly but only through measurements performed on the system. Explicitly, Pauli measurements $\{E_{\ell}\}_{\ell=1}^m$ are allowed to perform on the Gibbs state $\rho_{\beta} := e^{-\beta H} / \text{Tr}(e^{-\beta H})$ of the Hamiltonian H , and the measurement results are denoted by $\{e_{\ell}\}_{\ell=1}^m$, where $e_{\ell} = \text{Tr}(\rho_{\beta} E_{\ell})$. The learning task is to recover the coefficients $\boldsymbol{\mu} := (\mu_1, \dots, \mu_m)$ from measurement results. The work by Anshu et al. [13] uses Jaynes' principle [14] to formulate Hamiltonian learning task as an optimization program shown below:

$$\begin{aligned} \max_{\rho} \quad & S(\rho) \\ \text{s.t.} \quad & \text{Tr}(\rho E_{\ell}) = e_{\ell}, \forall \ell = 1, \dots, m \\ & \rho > 0, \text{Tr}(\rho) = 1. \end{aligned} \tag{1}$$

where $S(\rho) := -\text{Tr}(\rho \log \rho)$ is the von Neumann entropy and the maximization is over all quantum states. The authors show that the optimal state is exactly ρ_{β} and point out that the coefficients can be obtained by

solving its dual program defined as follows:

$$\boldsymbol{\mu} = \arg \min_{\boldsymbol{\nu}} \log Z_{\beta}(\boldsymbol{\nu}) + \beta \sum_{\ell=1}^m \nu_{\ell} e_{\ell}. \quad (2)$$

Here, $Z_{\beta}(\boldsymbol{\nu}) := \text{Tr}(e^{-\beta \sum_{\ell=1}^m \nu_{\ell} E_{\ell}})$ is the partition function and $\boldsymbol{\nu} := (\nu_1, \dots, \nu_m)$ is the vector consisting of all coefficients.

The strategy [13] implies that it suffices to solve the program to accomplish the Hamiltonian learning task. However, the challenge is to compute the logarithmic partition function (log-partition function, henceforth), since approximating partition functions of general Hamiltonians is #P hard [15, 16]. There are many quantum algorithms [17–23] for approximating partition functions, which are likely to require fault-tolerant quantum computers and are not suitable for our purpose. To overcome this challenge, we propose a hybrid quantum-classical log-partition function estimation framework by taking advantage of the system’s free energy properties and variational quantum algorithms (VQAs) [24]. The system’s free energy is defined by $F(\rho) := \text{Tr}(H\rho) - \beta^{-1}S(\rho)$ with the system being state ρ and inverse temperature β , whose global minimum is proportional to the log-partition function, i.e.,

$$\log \text{Tr}(e^{-\beta H}) = -\beta \min_{\rho} F(\rho). \quad (3)$$

Contributions. Utilizing this property and the VQAs framework, our approach computes the log-partition function via minimizing free energy. Explicitly, it is based on two steps: First, extracting Hamiltonian’s eigenvalues with NISQ computers via the combination of VQAs with importance sampling, which reduces the quantum resource requirement; Second, exploiting these eigenvalues to compute the free energy’s global minimum by classical convex optimization, with the advantage of avoidance of von Neumann entropy estimation. To these ends, our technical contributions are multi-folded and shown below.

- (i) We propose a hybrid quantum-classical Hamiltonian learning framework based on fundamental properties of free energy and utilize the following two subroutines: log-partition function estimation and stochastic Hamiltonian diagonalization.
- (ii) The main subroutine is the log-partition function estimation method, which combines the Hamiltonian diagonalization with classical convex optimization to minimize the free energy. Particularly, the minimization method avoids the von Neumann entropy estimation.
- (iii) We also propose a feasible scheme for Hamiltonian diagonalization by integrating variational quantum algorithms with the importance sampling technique.
- (iv) We finally demonstrate our algorithm’s validity by numerical simulations on several random Hamiltonians and many-body Hamiltonians (e.g., Ising model, XY model, and Heisenberg model).

Organization. In Sec. II, we review the Hamiltonian learning task and formally define the problems we resolved in this work; In Sec. III, we present the main results, including the Hamiltonian learning algorithm, log-partition function estimation, stochastic Hamiltonian diagonalization, and coefficient update procedure; In Sec. IV, we describe the experimental settings and provide numerical results for the Hamiltonian learning algorithm; Lastly, we conclude the paper in Sec. V. Proofs and more discussions are presented in the Supplementary Material.

II. PROBLEM STATEMENT

We consider quantum many-body systems consisting of qubits that are locally interacted with each other. Most physically relevant Hamiltonians have only a few-body interacted and are well described by an

expansion in a local Pauli basis. This means that the Hamiltonian H can be expanded in the following form:

$$H = \sum_{\ell=1}^m \mu_{\ell} E_{\ell}, \quad (4)$$

where $m = O(\text{poly}(n))$, $\boldsymbol{\mu} = (\mu_1, \dots, \mu_m) \in \mathbb{R}^m$ denotes the vector of interaction coefficients, and Pauli tensor products $E_{\ell} \in \{X, Y, Z, I\}^{\otimes n}$ only act non-trivially on κ or fewer qubits.

In the setting of Hamiltonian learning, the task is to learn the interaction coefficients $\boldsymbol{\mu}$ from the system's measurement results. One can access the measurement results of Gibbs state [10, 11] or a single eigenstate of the system [25]. In this paper, we assume that local measurements $\{E_{\ell}\}_{\ell=1}^m$ are performed on the Gibbs state $\rho_{\beta} := e^{-\beta H} / \text{Tr}(e^{-\beta H})$ at inverse temperature β . The measurement outcomes are denoted by $\{e_{\ell}\}_{\ell=1}^m$, given by

$$e_{\ell} = \text{Tr}(\rho_{\beta} E_{\ell}), \quad \forall \ell \in [m]. \quad (5)$$

Many approaches for obtaining local marginals $\{e_{\ell}\}_{\ell=1}^m$ have been proposed in the literature [26–28]. Thus, we assume these local marginals $\{e_{\ell}\}_{\ell=1}^m$ have already been given and focus on learning interaction coefficients from them. Formally, we define the Hamiltonian learning problem (HLP) as follows:

Definition 1 (HLP) *Consider a many-body Hamiltonian that has a decomposition given in Eq. (4) with $|\mu_{\ell}| \leq 1$ for all $\ell = 1, \dots, m$. Suppose we are given measurement outcomes $\{e_{\ell}\}_{\ell=1}^m$ of the quantum Gibbs state ρ_{β} , then the goal is to find an estimate $\hat{\boldsymbol{\mu}}$ of $\boldsymbol{\mu}$ such that*

$$\|\hat{\boldsymbol{\mu}} - \boldsymbol{\mu}\|_{\infty} \leq \epsilon, \quad (6)$$

where $\|\cdot\|_{\infty}$ norm means the maximal absolute value.

Recently, a variety of strategies for HLP are discovered for learning $\boldsymbol{\mu}$ from local measurements [10, 11, 13, 25, 29–31]. In this paper, we adopt the strategy proposed in Ref. [13]. This strategy takes the Jaynes' principle [14] to transform HLP into an optimization program. That is, finding a quantum state with the maximal entropy from all states whose measurement results under $\{E_{\ell}\}_{\ell=1}^m$ match $\{e_{\ell}\}_{\ell=1}^m$. Furthermore, the optimization program is formulated in Eq. (1). Particularly, in Ref. [14], it has shown that the optimal state is of the following form:

$$\sigma = \frac{\exp(-\beta \sum_{\ell=1}^m \mu_{\ell}^* E_{\ell})}{\text{Tr}(\exp(-\beta \sum_{\ell=1}^m \mu_{\ell}^* E_{\ell}))}. \quad (7)$$

The state σ is a quantum Gibbs state of a Hamiltonian that has interaction coefficients $\boldsymbol{\mu}^* = (\mu_1^*, \dots, \mu_m^*)$. An important result in Ref. [13] is that $\boldsymbol{\mu}^*$ is the target interaction coefficients, i.e., $\boldsymbol{\mu}^* = \boldsymbol{\mu}$. Especially, Ref. [13] pointed out one approach for obtaining $\boldsymbol{\mu}^*$ is to solve the optimization's dual program (cf. Eq (2)).

Notably, this approach's main obstacle is computing the log-partition function $\log Z_{\beta}(\boldsymbol{\nu})$. To overcome this challenge, our main task is to provide a practical approach for computing the log-partition function $\log Z_{\beta}(\boldsymbol{\nu})$ for arbitrary coefficients $\boldsymbol{\nu}$. Next, we define the log-partition function problem (LPFP) as follows:

Definition 2 (LPFP) *Given the system's Hamiltonian H and a constant $\beta > 0$, the goal is to find a number z such that*

$$|z - \log \text{Tr}(\exp(-\beta H))| \leq \epsilon. \quad (8)$$

In the following section, we introduce the solutions to HLP and LPFP that are implementable on NISQ computers.

III. MAIN RESULTS

The goal of this section is to introduce the main result of this paper. We first outline the hybrid quantum-classical Hamiltonian learning (HQHL) framework in Sec. III A and then discuss the main idea of our approach for computing log-partition function in Sec. III B. The rest discusses several subroutines for the HQHL algorithm.

A. Hamiltonian learning algorithm

For the Hamiltonian learning task, we introduce a practical hybrid quantum-classical framework, where the goal is to find the optimal coefficients via a gradient descent method with NISQ computers. In the framework (cf. Algorithm 1), a parameterized Hamiltonian $H(\boldsymbol{\nu}) := \sum_{\ell=1}^m \nu_{\ell} E_{\ell}$ with randomly chosen coefficients $\boldsymbol{\nu}$ is first taken to resemble the real Hamiltonian. Afterwards, the framework enters the training phase, where the coefficients $\boldsymbol{\nu}$ are trained to minimize the objective function $L(\boldsymbol{\nu})$, which is defined below:

$$L(\boldsymbol{\nu}) := \log Z_{\beta}(\boldsymbol{\nu}) + \beta \sum_{\ell=1}^m \nu_{\ell} e_{\ell}. \quad (9)$$

In the training process, the subroutine for Hamiltonian diagonalization (i.e., SVQE in Sec. III C) is first called to compute Hamiltonian's eigenvalues. Explicitly, a parameterized quantum circuit $U(\boldsymbol{\theta})$ is trained such that it can learn the eigenvectors of the Hamiltonian and output eigenvalues, which are evaluated via repeatedly preparing computational states, performing the parameterized quantum circuit $U(\boldsymbol{\theta})$, and measuring in observable $H(\boldsymbol{\nu})$. Then the log-partition function estimation (cf. Sec. III B) exploits these obtained eigenvalues to compute the objective function $L(\boldsymbol{\nu})$ and to obtain a probability distribution \mathbf{p}^* that consists of eigenvalues of the associated Gibbs state $\rho_{\beta}(\boldsymbol{\nu}) := e^{-\beta H(\boldsymbol{\nu})}/Z_{\beta}(\boldsymbol{\nu})$. Lastly, the coefficients are updated via a gradient descent method (cf. Sec. III D), where the previously obtained results (circuit $U(\boldsymbol{\theta})$ and distribution \mathbf{p}^*) are used to compute gradients $\nabla L(\boldsymbol{\nu})$. After the training process repeats sufficiently many times, the final coefficients $\boldsymbol{\nu}$ are supposed to approximate the target coefficients $\boldsymbol{\mu}$. A diagram for illustrating the HQHL algorithm is presented in Fig. 1.

Algorithm 1 Hybrid quantum-classical Hamiltonian learning algorithm (HQHL)

Input: Pauli operators $\{E_{\ell}\}_{\ell=1}^m$, coefficients $\{\nu_{\ell}\}_{\ell=1}^m$, constants $\{e_{\ell}\}_{\ell=1}^m$, constant β ;

Output: An estimate for target coefficients $\boldsymbol{\nu}$;

- 1: Set number of iterations I and $l = 1$;
- 2: Set parameterized quantum circuit $U(\boldsymbol{\theta})$;
- 3: Set learning rate r ;
- 4: **while** $l \leq I$ **do**
- 5: Set Hamiltonian $H(\boldsymbol{\nu}) = \sum_{\ell=1}^m \nu_{\ell} E_{\ell}$;
- 6: Train $U(\boldsymbol{\theta})$ by SVQE with $H(\boldsymbol{\nu})$;
- 7: Derive a probability \mathbf{p}^* by performing log-partition function estimation with $U(\boldsymbol{\theta})$ and β ;
- 8: Compute gradient $\nabla L(\boldsymbol{\nu})$ by subroutine gradient estimation with $U(\boldsymbol{\theta})$, \mathbf{p}^* , and β ;
- 9: Update coefficients $\boldsymbol{\nu} \leftarrow \boldsymbol{\nu} - r \nabla L(\boldsymbol{\nu})$;
- 10: Set $l \leftarrow l + 1$;

return the final coefficients $\boldsymbol{\nu}$.

Note that subroutines, including Hamiltonian diagonalization, log-partition function estimation, and coefficient update, could be implemented with NISQ devices. Thus our framework enables effective Hamiltonian learning on NISQ devices.

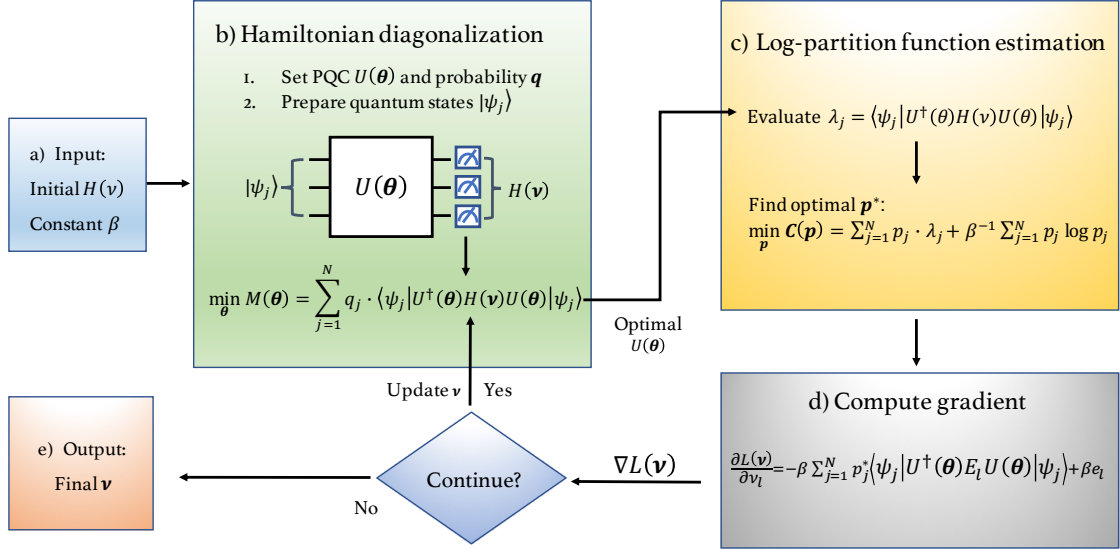


FIG. 1 The HQHL algorithm mainly consists of three steps. The step b) corresponds to select a parameterized quantum circuit that can diagonalize the parameterized Hamiltonian $H(\nu)$. Step c) concerns the evaluation of eigenvalues of $H(\nu)$ and optimization over the set of probability distributions to compute the log-partition function $\log Z_\beta(\nu)$. Step d) is to compute the objective function $L(\nu)$ and gradient $\nabla L(\nu)$. Then it determines whether continue to update the parameters ν . If yes, update the coefficients ν and go to step b); Otherwise, output the current ν as the approximate of the target coefficients.

B. Log-partition function estimation

In this section, we introduce a practical method to compute the log-partition function $\log Z_\beta(\nu)$. Motivating our method is the relationship between the log-partition function and free energy. Recall that free energy of the system being state ρ is given by $F(\rho) = \text{Tr}(H(\nu)\rho) - \beta S(\rho)$, assuming the system's Hamiltonian is $H(\nu)$. Then the relation is shown as follows:

$$\log Z_\beta(\nu) = -\beta \min_{\rho} F(\rho). \quad (10)$$

The relation in Eq. (10) suggests an approach for computing the log-partition function $\log Z_\beta(\nu)$, that is, solving the optimization program on Eq. (10)'s right-hand side. However, it is infeasible to minimize the free energy directly since performing entropy estimation with NISQ devices is difficult [32]. To deal with this issue, we choose an alternate version of Eq. (10):

$$\log Z_\beta(\nu) = -\beta \min_{\mathbf{p}} \left(\sum_{j=1}^N p_j \cdot \lambda_j + \beta^{-1} \sum_{j=1}^N p_j \log p_j \right), \quad (11)$$

where $\lambda = (\lambda_1, \dots, \lambda_N)$ is the vector of eigenvalues of $H(\nu)$, and $\mathbf{p} = (p_1, \dots, p_N)$ represents a probability distribution with N the Hamiltonian's dimension. Following the equality in Eq. (11), our task is to solve the following optimization program:

$$\begin{aligned} \min_{\mathbf{p}} \quad & C(\mathbf{p}) \\ \text{s.t.} \quad & \sum_{j=1}^N p_j = 1 \\ & p_j \geq 0, \forall j = 1, \dots, N \end{aligned} \quad (12)$$

where $C(\mathbf{p}) = \sum_{j=1}^N p_j \cdot \lambda_j + \beta^{-1} \sum_{j=1}^N p_j \log p_j$.

The optimization program in Eq. (12) is a typical convex optimization program. There are many classical algorithms to solve the program, such as the interior-point method [33], ellipsoid method [34], cutting-plane method [35], and random walks [36], etc. In this paper, we consider using the cutting plane method [37, 38], where the membership and evaluation procedures are required [39]. Regarding the program in Eq. (12), the membership procedure determines whether a point belongs to the set of probability distributions. The evaluation procedure takes in a probability distribution \mathbf{p} and returns the value $C(\mathbf{p})$ with high accuracy. Notably, it is easy to determine whether the given point is a probability distribution but challenging to efficiently evaluate the function value. In the following, we will describe our approach in detail for solving this program, which can then compute the partition function (cf. Algorithm 2).

Algorithm 2 Log-partition function estimation

Input: Parameterized quantum circuit $U(\boldsymbol{\theta})$, Hamiltonian $H(\boldsymbol{\nu})$, constant β ;

Output: An estimate for $\log Z_\beta(\boldsymbol{\nu})$;

1: # Evaluation procedure construction

2: Take probability distribution \mathbf{p} as input;

3: Set integer T and D ;

4: Sample TD integers $t_1^1, \dots, t_T^1, \dots, t_1^D, \dots, t_T^D$ according to \mathbf{p} ;

5: Prepare computational states $|\psi_{t_1^1}\rangle, \dots, |\psi_{t_T^1}\rangle, \dots, |\psi_{t_1^D}\rangle, \dots, |\psi_{t_T^D}\rangle$;

6: Compute approximate eigenvalues $\lambda_{t_j^s} = \langle \psi_{t_j^s} | U^\dagger(\boldsymbol{\theta}) H(\boldsymbol{\nu}) U(\boldsymbol{\theta}) | \psi_{t_j^s} \rangle$ for all $j = 1, \dots, T$ and $s = 1, \dots, D$;

7: Compute averages: $ave_s = \frac{1}{T} \sum_{j=1}^T \lambda_{t_j^s}$ for all $s = 1, \dots, D$;

8: Compute function value $C(\mathbf{p}) \leftarrow \text{median}(\lambda_{ave_1}, \dots, \lambda_{ave_D}) + \beta^{-1} \sum_{j=1}^N p_j \log p_j$;

9: # Membership procedure construction

10: Construct a membership procedure;

11: # Convex optimization solution

12: Compute the function's global minimum value $C(\mathbf{p}^*)$ and the optimal point \mathbf{p}^* via the cutting plane method.

return value $-\beta C(\mathbf{p}^*)$ and the final point \mathbf{p}^* .

Algorithm 2 computes the log-partition function using a classical convex optimization method, where the key is to construct the evaluation procedure. Concretely, it first shows the construction process of evaluation procedure, that is, given a point \mathbf{p} , find an estimate for $C(\mathbf{p})$, where the main task is how to efficiently evaluate $\sum_j p_j \lambda_j$, given access to eigenvalues λ_j . Specifically, we use the importance sampling technique (cf. lines 3-8) to do this, i.e., i) we sample TD indices according to \mathbf{p} (cf. line 4); ii) we evaluate these associated eigenvalues via a parameterized quantum circuit $U(\boldsymbol{\theta})$ which can diagonalize the Hamiltonian $H(\boldsymbol{\nu})$ (cf. lines 5-6); iii) we take the average over T (cf. line 7) and the median over D (cf. line 8) to evaluate the function value $C(\mathbf{p})$ with high accuracy and success probability, respectively. Then, with the evaluation procedure and the membership procedure, the global minimum of $C(\mathbf{p})$ could be obtained via the cutting plane method [37–39]. Based on the relationship between $\log Z_\beta(\boldsymbol{\nu})$ and $C(\mathbf{p}^*)$, i.e., Eq. (11), we could derive the log-partition function value.

Since the efficiency of Algorithm 2 mainly relies on the cost of the evaluation procedure, we discuss it here. Suppose we have access to Hamiltonian $H(\boldsymbol{\nu})$'s eigenvalues $\boldsymbol{\lambda}$, then the objective function $C(\mathbf{p})$ can be effectively evaluated on NISQ computers. Recall that $C(\mathbf{p})$ contains two parts $\sum_{j=1}^N p_j \cdot \lambda_j$ and $\beta^{-1} \sum_{j=1}^N p_j \log p_j$. On the one hand, value $\beta \sum_{j=1}^N p_j \log p_j$ can be computed immediately since \mathbf{p} is stored on classical devices. On the other hand, value $\sum_{j=1}^N p_j \cdot \lambda_j$ can be regarded as an expectation of probability \mathbf{p} . That is, value λ_j is sampled with probability p_j . Usually, the expectation can be approximated by the sampling mean based on Chebyshev's inequality and Chernoff bounds. By Chebyshev's inequality, the expectation can be estimated up to precision ϵ with high probability (e.g., larger than $2/3$) by taking $T = O(m \|\boldsymbol{\nu}\|_2^2 / \epsilon^2)$ samples, since the variance is bounded by the squared spectral norm of $H(\boldsymbol{\nu})$, which is less than $\sqrt{m} \|\boldsymbol{\nu}\|_2$ (cf. Lemma S1). Chernoff bounds allow improving success probability to $1 - \eta$ at

an additional cost of a multiplicative factor of $D = O(\log(1/\eta))$. Now we present the number of required samples for evaluation in Proposition 1.

Proposition 1 *For any constant $\beta > 0$ and parameterized Hamiltonian $H(\boldsymbol{\nu}) = \sum_{\ell=1}^m \nu_\ell E_\ell$ with $E_\ell \in \{X, Y, Z, I\}^{\otimes n}$ and $\boldsymbol{\nu} \in \mathbb{R}^m$, suppose we are given access to a parameterized quantum circuit $U(\boldsymbol{\theta})$ that can prepare $H(\boldsymbol{\nu})$'s eigenvectors, then the objective function $C(\mathbf{p})$ can be computed up to precision ϵ with probability larger than $2/3$ by taking $T = O(m\|\boldsymbol{\nu}\|_2^2/\epsilon^2)$ samples. Furthermore, the probability can be improved to $1 - \eta$ costing an additional multiplicative factor of $D = O(\log(1/\eta))$.*

Notably, the number of samples is irrelevant to the dimension, implying that our evaluation method is computationally efficient. At last, to complement the assumption, we provide a procedure for extracting eigenvalues in the next section, *stochastic Hamiltonian diagonalization*. Consequently, after Hamiltonian diagonalization, we will obtain a parameterized quantum circuit $U(\boldsymbol{\theta})$ that can learn Hamiltonian's eigenvectors and output eigenvalues.

C. Stochastic Hamiltonian diagonalization

Diagonalizing Hamiltonians is crucial in exploring the quantum system's physical properties. Some known quantum algorithms for Hamiltonian diagonalization are based on quantum fast Fourier transform [40], which may be too costly for NISQ computers and thus not suitable for our purpose. Recently, there have already been some works on finding ground and excited eigenstates of the Hamiltonian with NISQ devices, i.e., variational quantum eigensolvers [41–47]. This section presents a *Stochastic Variational Quantum Eigensolver* (SVQE), which follows a similar idea of the work by Nakanishi, Mitarai, and Fujii [44]. The fundamental of SVQE is eigenvalues' variational property, i.e., the eigenvalues majorize the diagonal elements, and the dot function with an increasingly ordered vector is Schur concave [48] (see more discussions in Sec. A 1 a). In contrast, we choose a probability distribution as the vector and then uses importance sampling to reduce the quantum resources, such as the number of measurements.

To diagonalize Hamiltonians, SVQE employs a parameterized quantum circuit (PQC) $U(\boldsymbol{\theta})$ and computational bases, denoted by $|\psi_1\rangle, \dots, |\psi_N\rangle$, to generate parameterized ansatzes $U(\boldsymbol{\theta})|\psi_1\rangle, \dots, U(\boldsymbol{\theta})|\psi_N\rangle$, and then trains the PQC $U(\boldsymbol{\theta})$ by minimizing the objective function $M(\boldsymbol{\theta})$, given below:

$$M(\boldsymbol{\theta}) := \sum_{j=1}^N q_j \cdot \langle \psi_j | U^\dagger(\boldsymbol{\theta}) H(\boldsymbol{\nu}) U(\boldsymbol{\theta}) | \psi_j \rangle, \quad (13)$$

where $\mathbf{q} = (q_1, \dots, q_N)$ is a probability distribution with $q_1 < q_2 < \dots < q_N$. In the training process, parameters $\boldsymbol{\theta}$ are updated via the parameter shift rule [49], which indicates that gradient can be computed via loss evaluation $M(\boldsymbol{\theta})$. However, for large Hamiltonians, computing $M(\boldsymbol{\theta})$ can be daunting since there are exponentially many values $\langle \psi_j | U^\dagger(\boldsymbol{\theta}) H(\boldsymbol{\nu}) U(\boldsymbol{\theta}) | \psi_j \rangle$ that need to be estimated. To overcome this challenge, we use the importance sampling technique to reduce the number of required values. Subsequently, after training, a PQC $U(\boldsymbol{\theta}_{opt})$ with optimal parameters $\boldsymbol{\theta}_{opt}$ will be obtained that can learn the eigenvectors of Hamiltonian $H(\boldsymbol{\nu})$ and output eigenvalues. The details of SVQE are shown in Algorithm 3.

Algorithm 3 Stochastic variational quantum eigensolver (SVQE)

Input: Parameterized quantum circuit $U(\boldsymbol{\theta})$, Hamiltonian $H(\boldsymbol{\nu})$;

Output: Optimal PQC $U(\boldsymbol{\theta})$;

- 1: Set number of iterations I and $l = 1$;
- 2: Set integers T and D ;
- 3: Set learning rate r_θ ;
- 4: Set probability distribution \mathbf{q} ;
- 5: Sample TD integers $k_1^1, \dots, k_T^1, \dots, k_1^D, \dots, k_T^D$ according to \mathbf{q} ;
- 6: Prepare computational states $|\psi_{k_1^1}\rangle, \dots, |\psi_{k_T^1}\rangle, \dots, |\psi_{k_1^D}\rangle, \dots, |\psi_{k_T^D}\rangle$;
- 7: **while** $l \leq I$ **do**
- 8: Compute value $\langle \psi_{k_j^s} | U^\dagger(\boldsymbol{\theta}) H(\boldsymbol{\nu}) U(\boldsymbol{\theta}) | \psi_{k_j^s} \rangle$ for all $j = 1, \dots, T$ and $s = 1, \dots, D$;
- 9: Compute averages: $ave_s = \frac{1}{T} \sum_{j=1}^T \langle \psi_{k_j^s} | U^\dagger(\boldsymbol{\theta}) H(\boldsymbol{\nu}) U(\boldsymbol{\theta}) | \psi_{k_j^s} \rangle$ for all $s = 1, \dots, D$;
- 10: Let $M(\boldsymbol{\theta}) \leftarrow \text{median}(ave_1, \dots, ave_D)$;
- 11: Use $M(\boldsymbol{\theta})$ to compute the gradient ∇ by parameter shift rules [49];
- 12: Update parameters $\boldsymbol{\theta} \leftarrow \boldsymbol{\theta} - r_\theta \nabla$;
- 13: Set $l \leftarrow l + 1$;

return the final $U(\boldsymbol{\theta})$.

In Algorithm 3, function $M(\boldsymbol{\theta})$ is evaluated in a random way, since $M(\boldsymbol{\theta})$ can be regarded as an expectation of probability distribution \mathbf{q} . The number of samples is determined by the accuracy ϵ and Hamiltonian $H(\boldsymbol{\nu})$. By Chebyshev's inequality, estimating $M(\boldsymbol{\theta})$ up to precision ϵ with high probability requires $T = O(m\|\boldsymbol{\nu}\|_2^2/\epsilon^2)$ samples, since the variance is bounded by the spectral norm, which is less than $\sqrt{m}\|\boldsymbol{\nu}\|_2$ (cf. Lemma S1). Meanwhile, the expectation value $\langle \psi_j | U^\dagger(\boldsymbol{\theta}) H(\boldsymbol{\nu}) U(\boldsymbol{\theta}) | \psi_j \rangle$ is evaluated by measurements. Our approach computes the expectation value of the observable $H(\boldsymbol{\nu})$ by measuring each Pauli operator E_ℓ separately, since there are only $m = O(\text{poly}(n))$ Pauli operators (cf. Lemma S2). Some other methods for computing expectation value of Hamiltonians can be found in Ref. [50, 51], where importance sampling is employed to sample Pauli operator E_ℓ of the Hamiltonian. At last, the number of required samples and measurements for evaluation is presented in Proposition 2.

Proposition 2 Consider a parameterized Hamiltonian $H(\boldsymbol{\nu}) = \sum_{\ell=1}^m \nu_\ell E_\ell$ with Pauli operators $E_\ell \in \{X, Y, Z, I\}^{\otimes n}$ and constants $\nu_\ell \in [-1, 1]$. Given any constants $\epsilon > 0$, $\eta \in (0, 1)$, $\beta > 0$, the objective function $M(\boldsymbol{\theta})$ in SVQE can be estimated up to precision ϵ with probability at least $1 - \eta$, costing TD samples with $T = O(m\|\boldsymbol{\nu}\|_2^2/\epsilon^2)$ and $D = O(\log(1/\eta))$. Besides, the total number of measurements is given below:

$$O\left(\frac{mTD\|\boldsymbol{\nu}\|_1^2(n + \log(m/\eta))}{\epsilon^2}\right). \quad (14)$$

It is easy to see that the number of measurements is irrelevant to the system's dimension. Thus, SVQE significantly reduces the number of measurements and could be applied on NISQ computers.

D. Coefficients update

The last step of the HQHL algorithm is to update the coefficients $\boldsymbol{\nu}$ of the objective function $L(\boldsymbol{\nu})$. Here, we employ a gradient-based method to do the optimization. Thus it is essential to efficiently compute the gradient $\nabla L(\boldsymbol{\nu})$. Using the gradient, parameters are updated in the following way:

$$\boldsymbol{\nu} \leftarrow \boldsymbol{\nu} - r \nabla L(\boldsymbol{\nu}), \quad (15)$$

where r is the learning rate. The expression of the gradient is shown below:

$$\nabla L(\boldsymbol{\nu}) = \left(\frac{\partial L(\boldsymbol{\nu})}{\partial \nu_1}, \dots, \frac{\partial L(\boldsymbol{\nu})}{\partial \nu_m} \right). \quad (16)$$

Furthermore, the explicit formula of each partial derivative is given in Ref. [13]:

$$\frac{\partial L(\boldsymbol{\nu})}{\partial \nu_\ell} = \frac{\partial}{\partial \nu_\ell} \log Z_\beta(\boldsymbol{\nu}) + \beta e_\ell = -\beta \text{Tr}(\rho_\beta(\boldsymbol{\nu}) E_\ell) + \beta e_\ell, \quad (17)$$

where $\rho_\beta(\boldsymbol{\nu}) = e^{-\beta H(\boldsymbol{\nu})}/Z_\beta(\boldsymbol{\nu})$ represents the parameterized Gibbs state.

According to the second equality in Eq. (17), it seems that preparing the Gibbs state $\rho_\beta(\boldsymbol{\nu})$ is necessary to compute the gradient. However, preparing Gibbs state on NISQ devices is hard [52–56]. To overcome this challenge, we present a procedure for gradient estimation without preparing the Gibbs state $\rho_\beta(\boldsymbol{\nu})$.

Recall that the SVQE algorithm can provide information about eigenvectors of $\rho_\beta(\boldsymbol{\nu})$. Ideally, SVQE can output a parameterized quantum circuit $U(\boldsymbol{\theta})$ that prepares $H(\boldsymbol{\nu})$ and $\rho_\beta(\boldsymbol{\nu})$'s eigenvectors because $H(\boldsymbol{\nu})$ and $\rho_\beta(\boldsymbol{\nu})$ are commuting. Meanwhile, the developed tools for computing the log-partition function can be used to compute $\rho_\beta(\boldsymbol{\nu})$'s eigenvalues. The reason is that the optimum $\hat{\mathbf{p}}^*$ in Algorithm 2 consists of $\rho_\beta(\boldsymbol{\nu})$'s eigenvalues (A proof for this fact can be found in Sec. B 1). Let $U(\boldsymbol{\theta})$ denote the obtained PQC from SVQE and $\hat{\mathbf{p}}^*$ denote the optimal probability distribution from Algorithm 2. Then the partial derivative can be computed in the sense that

$$\frac{\partial L(\boldsymbol{\nu})}{\partial \nu_\ell} \approx -\beta \sum_{j=1}^N \hat{p}_j^* \cdot \langle \psi_j | U^\dagger(\boldsymbol{\theta}) E_\ell U(\boldsymbol{\theta}) | \psi_j \rangle + \beta e_\ell. \quad (18)$$

The validity of this relation is proved in Proposition 3.

Proposition 3 (Correctness) Consider a parameterized Hamiltonian $H(\boldsymbol{\nu})$ and its Gibbs state $\rho_\beta(\boldsymbol{\nu})$. Suppose the $U(\boldsymbol{\theta})$ from SVQE (cf. Algorithm 3) and $\hat{\mathbf{p}}^*$ from log-partition function estimation procedure (cf. Algorithm 2) are optimal. Define a density operator ρ_β^* as follows:

$$\rho_\beta^* := \sum_{j=1}^N \hat{p}_j^* \cdot U(\boldsymbol{\theta}) | \psi_j \rangle \langle \psi_j | U^\dagger(\boldsymbol{\theta}). \quad (19)$$

where $\{|\psi_j\rangle\}$ denote the computational basis. Denote the estimated eigenvalues by $\hat{\boldsymbol{\lambda}}$, where $\hat{\lambda}_j = \langle \psi_j | U^\dagger(\boldsymbol{\theta}) H(\boldsymbol{\nu}) U(\boldsymbol{\theta}) | \psi_j \rangle$. Then, ρ_β^* is an approximate of $\rho_\beta(\boldsymbol{\nu})$ in the sense that

$$D(\rho_\beta^*, \rho_\beta(\boldsymbol{\nu})) \leq \sqrt{2\beta \|\hat{\boldsymbol{\lambda}} - \boldsymbol{\lambda}\|_\infty}. \quad (20)$$

where $D(\cdot, \cdot)$ denotes the trace distance, $\boldsymbol{\lambda}$ represent $H(\boldsymbol{\nu})$'s true eigenvalues.

Algorithm 4 Gradient estimation

Input: Post-training circuit $U(\boldsymbol{\theta})$, Pauli operators $\{E_\ell\}_{\ell=1}^m$, optimal $\hat{\mathbf{p}}^*$, and constants β and $\{e_\ell\}_{\ell=1}^m$;

Output: Gradient estimate $\nabla L(\boldsymbol{\nu})$;

- 1: Set $\ell = 1$;
- 2: Set integer K and D ;
- 3: Sample K integers $l_1^1, \dots, l_K^1, \dots, l_1^D, \dots, l_K^D$, according to $\hat{\mathbf{p}}^*$;
- 4: Prepare computational states $|\psi_{l_1^1}\rangle, \dots, |\psi_{l_K^1}\rangle, \dots, |\psi_{l_1^D}\rangle, \dots, |\psi_{l_K^D}\rangle$;
- 5: **while** $\ell \leq m$ **do**
- 6: Compute value $\langle \psi_{l_j^s} | U^\dagger(\boldsymbol{\theta}) E_\ell U(\boldsymbol{\theta}) | \psi_{l_j^s} \rangle$ for $j = 1, \dots, K$ and $s = 1, \dots, D$;
- 7: Compute averages: $ave_s = \frac{1}{K} \sum_{j=1}^K \langle \psi_{l_j^s} | U^\dagger(\boldsymbol{\theta}) E_\ell U(\boldsymbol{\theta}) | \psi_{l_j^s} \rangle$ for all $s = 1, \dots, D$;
- 8: Compute value $s_\ell = -\beta \cdot \text{median}(ave_1, \dots, ave_D) + \beta e_\ell$;
- 9: Set $\ell \leftarrow \ell + 1$;

return vector (s_1, \dots, s_m) .

Three aspects	# qubits	# μ	β	LR	μ	E_ℓ
	3	3	1	1.0	[0.3408 -0.6384 -0.4988]	[[0 2 1] [2 1 3] [0 3 3]]
Vary β	3	3	0.3	8.0	[-0.4966 -0.8575 -0.7902]	[[1 0 0] [3 0 2] [3 1 3]]
			3	0.1	[0.5717 -0.1313 0.2053]	[[1 0 0] [3 3 3] [0 2 3]]
Vary # μ	3	4	1	1.0	[-0.7205 -0.3676 -0.7583 -0.3002]	[[3 2 1] [2 1 3] [0 0 2] [2 0 0]]
		5			[-0.5254 -0.1481 -0.0037 -0.4373 0.7326]	[[1 3 0] [2 1 1] [3 3 2] [2 3 1] [0 2 0]]
		6			[-0.5992 0.7912 0.5307 -0.5422 -0.9239 0.0354]	[[3 2 2] [0 2 1] [1 2 1] [2 2 0] [0 1 2] [3 2 1]]
Vary # qubits	4	3	1	1.0	[0.0858 0.3748 -0.1007]	[[0 2 0 1] [1 0 0 1] [2 0 1 0]]
	5				[-0.0411 0.7882 0.6207]	[[2 2 2 1 2] [2 3 3 2 1] [1 2 0 2 3]]

TABLE I Hyper-parameters setting. The number of qubits (# qubits) varies from 3 to 5, and the number of μ (# μ) from 3 to 6. β is chosen as 0.3, 1, 3. “LR” denotes learning rate. The values of μ are sampled uniformly in the range of $[-1, 1]$. The term, likes “[[0 2 1] [2 1 3] [0 3 3]]”, indicates there are three E_ℓ ’s and each has three qubits with the corresponding Pauli tensor product. Here “0,1,2,3” represent “I, X, Y, Z” respectively. For example, for the first sample, the corresponding Hamiltonian is taken as $H=0.3408 \cdot I \otimes Y \otimes X -0.6384 \cdot Y \otimes X \otimes Z -0.4988 \cdot I \otimes Z \otimes Z$.

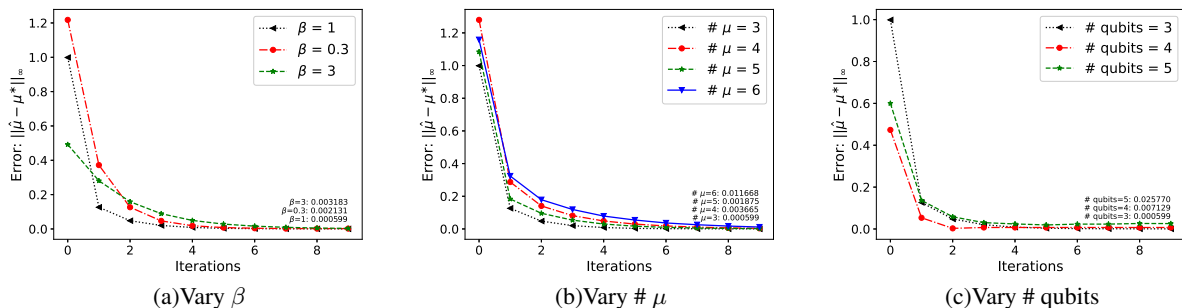


FIG. 2 The curves for the infinity norm of the error of μ with (a) different β , (b) different number of μ and (c) different number of qubits. The numbers on the line represent the values of the last iteration. These numbers close to 0 indicate that our algorithm is effective.

Now we provide the gradient estimation procedure in Algorithm 4. Explicitly, each component of the gradient is evaluated by repeatedly preparing computational states $|\psi_j\rangle$ and performing circuit $U(\theta)$, and then measuring in Pauli operator E_ℓ . Since the $\sum_j \tilde{p}_j^* \cdot \langle \psi_j | U^\dagger(\theta) E_\ell U(\theta) | \psi_j \rangle$ is framed as an expectation, thus it is also computed via sampling. Particularly, the sample complexity is provided in Proposition 4. It is easy to see that complexity scales polynomially in n , β , and ϵ , implying that estimation is computationally efficient.

Proposition 4 (Sample complexity) *Given $\epsilon > 0$ and $\eta \in (0, 1)$, Algorithm 4 can compute an estimate for the gradient $\nabla L(\nu)$ up to precision ϵ with probability larger than $1 - \eta$. Particularly, the overall number of samples is $KD = O(\beta^2 \log(2m/\eta)/\epsilon^2)$ with $K = O(\beta^2/\epsilon^2)$ and $D = O(\log(2m/\eta))$. Besides, the total number of measurements is $O(KD \cdot m\beta^2(n + \log(m/\eta))/\epsilon^2)$.*

IV. NUMERICAL RESULTS

A. Random Hamiltonian models

In order to detect the practical performance of our method, we conduct several numerical experiments to verify its effectiveness with random Hamiltonians. Concretely, we verify our method mainly from three

Many-body models	# qubits	# μ	β	LR	μ
Ising model	3	6	1.0	2.0	$[J_0 = 0.1981, h_0 = 0.7544]$
	4	8		1.0	$[J_0 = 0.5296, h_0 = 0.4996]$
	5	10		0.5	$[J_0 = -0.6916, h_0 = 0.4801]$
XY model	3	6	1.0	1.0	$J_1 = -0.0839$
	4	8		1.0	$J_1 = 0.2883$
	5	10		0.6	$J_1 = -0.7773$
Heisenberg model	3	12	1.0	1.0	$[J_2 = 0.0346, h_2 = 0.8939]$
	4	16		1.0	$[J_2 = -0.5831, h_2 = -0.0366]$
	5	20		1.0	$[J_2 = 0.2883, h_2 = -0.2385]$

TABLE II Hyper-parameters setting for many-body models. For each Hamiltonian model, the number of qubits varies from 3 to 5, and the number of μ is determined by the number of Pauli operators. “LR” denotes learning rate. The values of μ are sampled uniformly in the range of $[-1, 1]$.

aspects: different β , different number of μ (# μ) and different number of qubits (# qubits).

In the experimental setting, we randomly choose Pauli tensor products E_ℓ from $\{X, Y, Z, I\}^{\otimes n}$ and target coefficients μ from a uniform distribution in $[-1, 1]$. Specifically, we first vary the values of β by fixing the number of μ and the number of qubits to explore our method’s sensitivity to temperature. We similarly vary the number of μ and the number of qubits by fixing other hyper-parameters to explore our method’s scalability. The actual values of these hyper-parameters sampled/chose in each trial are concluded in Table I. The variational quantum circuit $U(\theta)$ for the subroutine stochastic variational quantum eigensolver (SVQE) is selected in Fig. 3. And the update process is greatly similar to the original variational quantum eigensolver [41]. Hence, we omit the detailed hyper-parameter settings for this subroutine.

The results for these three aspects are illustrated in Fig. 2. We find that all curves converge to the values close to 0 in less than ten iterations, which shows our method is effective. Specifically, our method works for different β means that it is robust to temperature. And the efficacy of the number of μ and the number of qubits reveals our method’s scalability to a certain extent.

B. Quantum many-body models

As Hamiltonian learning’s main application is to recover the many-body Hamiltonians, we demonstrate the performance of our algorithm for quantum many-body models. Particularly, we consider the one-dimensional nearest-neighbor Ising model, XY model, and Heisenberg model. These many-body models

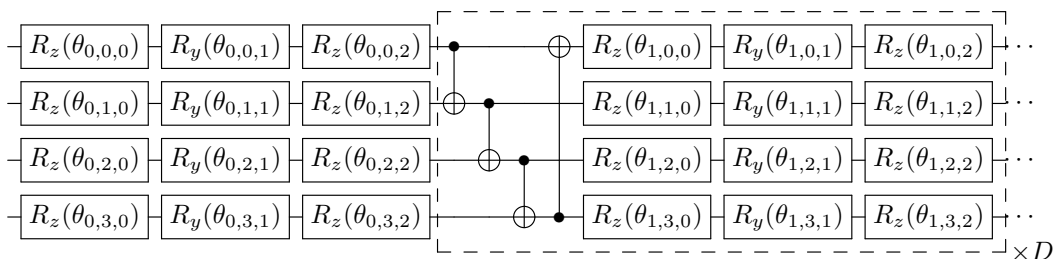


FIG. 3 The selected quantum circuit $U(\theta)$ for statistical variational quantum eigensolver (SVQE). Here, D represents circuit depth and we choose $D = 10, 20, 40$ for 3, 4, 5 qubits, respectively. θ are randomly initialized from a uniform distribution in $[0, 2\pi]$ and updated via gradient descent method.

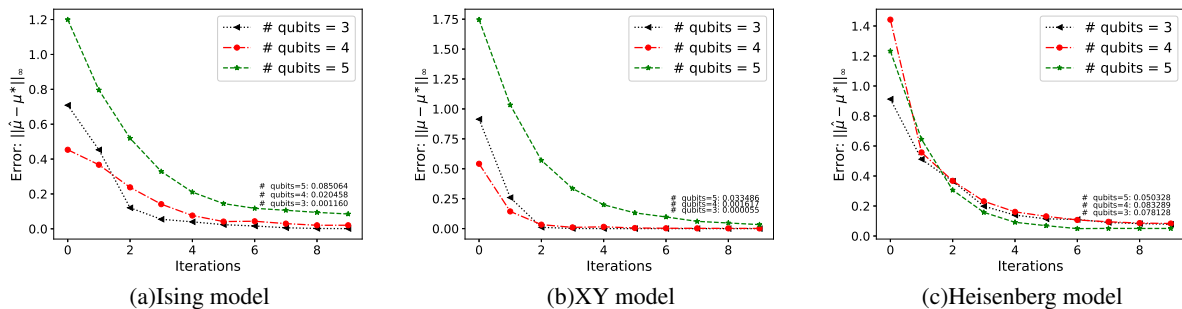


FIG. 4 The curves for the infinity norm of the error of μ for different many-body Hamiltonians. For each model, the number of qubits varies from 3 to 5. The numbers on the line represent the values of the last iteration. These numbers close to 0 demonstrate the algorithm’s performance for many-body Hamiltonians.

are described by the Hamiltonians shown below:

$$\text{(Ising model)} \quad H_0 = J_0 \sum_{l=1}^n Z^l Z^{l+1} + h_0 \sum_{l=1}^n X^l, \quad (21)$$

$$\text{(XY model)} \quad H_1 = J_1 \sum_{l=1}^n (X^l X^{l+1} + Y^l Y^{l+1}), \quad (22)$$

$$\text{(Heisenberg model)} \quad H_2 = J_2 \sum_{l=1}^n (X^l X^{l+1} + Y^l Y^{l+1} + Z^l Z^{l+1}) + h_2 \sum_{l=1}^n Z^l, \quad (23)$$

where periodic boundary conditions are assumed (i.e., $X^{n+1} = X^1$, $Y^{n+1} = Y^1$, and $Z^{n+1} = Z^1$). Coefficient J is the coupling constant for the nearest neighbor interaction, and h represents the external transverse magnetic field.

The experimental parameters are concluded in Table II. We consider the models with a different number of qubits and set the inverse temperature $\beta = 1$. The coefficients J_0, J_1, J_2 and h_0, h_2 are sampled uniformly from a uniform distribution on $[-1, 1]$. We also employ the parameterized quantum circuit $U(\theta)$ in Fig. 3 for the SVQE. The numerical results can be found in Fig. 4, which imply our method is applicable to recover quantum many-body Hamiltonians.

V. CONCLUSION

To summarize, we have presented a hybrid quantum-classical algorithm for Hamiltonian learning on NISQ devices. We achieve this purpose by developing two key subroutines: stochastic variational quantum eigensolver (SVQE) and log-partition function estimation. Explicitly, the former utilizes the parameterized quantum circuit to learn the eigenvectors of the Hamiltonian and output eigenvalues. Then, the latter exploits the obtained eigenvalues with the classical convex optimization to minimize the free energy, where von Neumann entropy estimation is no longer necessary. Furthermore, we have demonstrated the validity of our algorithm for random Hamiltonian models as well as many-body Hamiltonian models with interest in quantum physics.

We believe our approach would have capabilities of many future directions. For example, 1) SVQE might enrich the VQE family in the fields of molecules and materials; 2) As many problems in computer science can be framed as partition function problems, including counting coloring, and matchings, our method could contribute to these fields as well. Furthermore, it is reasonable to explore our algorithm’s applications in quantum machine learning [57], quantum error correction [58], and tomography [9].

Acknowledgements

Y. W. and G. L. acknowledge support from the Australian Research Council (Grant No: DP180100691) and the Baidu-UTS AI Meets Quantum project. G. L. acknowledges the financial support from China Scholarship Council (No. 201806070139).

-
- [1] D. Gross, Y.-K. Liu, S. T. Flammia, S. Becker, and J. Eisert, *Physical Review Letters* **105**, 150401 (2010), [arXiv:0909.3304](#) .
- [2] M. P. da Silva, O. Landon-Cardinal, and D. Poulin, *Physical Review Letters* **107**, 210404 (2011), [arXiv:1104.3835](#) .
- [3] N. Wiebe, C. Granade, C. Ferrie, and D. G. Cory, *Physical Review Letters* **112**, 190501 (2014), [arXiv:1309.0876](#) .
- [4] N. Wiebe, C. Granade, C. Ferrie, and D. Cory, *Physical Review A - Atomic, Molecular, and Optical Physics* **89**, 1 (2014), [arXiv:1311.5269](#) .
- [5] J. Preskill, *Quantum* **2**, 79 (2018), [arXiv:1801.00862](#) .
- [6] C. Di Franco, M. Paternostro, and M. S. Kim, *Physical Review Letters* **102**, 187203 (2009), [arXiv:0812.3510](#) .
- [7] Y. Wang, D. Dong, B. Qi, J. Zhang, I. R. Petersen, and H. Yonezawa, *IEEE Transactions on Automatic Control* **63**, 1388 (2018), [arXiv:1610.08841](#) .
- [8] A. Sone and P. Cappellaro, *Physical Review A* **96**, 062334 (2017), [arXiv:1702.03280](#) .
- [9] M. Kieferová and N. Wiebe, *Physical Review A* **96**, 062327 (2017), [arXiv:arXiv:1612.05204v1](#) .
- [10] E. Bairey, I. Arad, and N. H. Lindner, *Physical Review Letters* **122**, 1 (2019), [arXiv:1807.04564](#) .
- [11] T. J. Evans, R. Harper, and S. T. Flammia, (2019), [arXiv:1912.07636](#) .
- [12] C. E. Granade, C. Ferrie, N. Wiebe, and D. G. Cory, *New Journal of Physics* **14**, 103013 (2012), [arXiv:1207.1655](#) .
- [13] A. Anshu, S. Arunachalam, T. Kuwahara, and M. Soleimanifar, (2020), [arXiv:2004.07266](#) .
- [14] E. T. Jaynes, *Physical review* **106**, 620 (1957).
- [15] P. M. Long and R. A. Servedio, (2010).
- [16] L. A. Goldberg and M. Jerrum, *Information and Computation* **206**, 908 (2008).
- [17] D. Štefankovič, S. Vempala, and E. Vigoda, *Journal of the ACM* **56**, 1 (2009).
- [18] P. Wocjan, C.-F. Chiang, D. Nagaj, and A. Abeyesinghe, *Physical Review A* **80**, 022340 (2009), [arXiv:arXiv:0811.0596v3](#) .
- [19] A. Montanaro, *Proceedings of the Royal Society A: Mathematical, Physical and Engineering Sciences* **471**, 20150301 (2015), [arXiv:1504.06987](#) .
- [20] D. Poulin and P. Wocjan, *Physical Review Letters* **103**, 1 (2009), [arXiv:0905.2199](#) .
- [21] A. N. Chowdhury, R. D. Somma, and Y. Subasi, , 1 (2019), [arXiv:1910.11842](#) .
- [22] A. W. Harrow and A. Y. Wei, , 1 (2019), [arXiv:1907.09965](#) .
- [23] S. Arunachalam, V. Havlicek, G. Nannicini, K. Temme, and P. Wocjan, , 1 (2020), [arXiv:2009.11270](#) .
- [24] M. Cerezo, A. Poremba, L. Cincio, and P. J. Coles, *Quantum* **4**, 248 (2020), [arXiv:1906.09253](#) .
- [25] X.-L. Qi and D. Ranard, *Quantum* **3**, 159 (2017), [arXiv:1712.01850](#) .
- [26] J. Cotler and F. Wilczek, *Physical Review Letters* **124** (2020), 10.1103/PhysRevLett.124.100401, [arXiv:1908.02754](#) .
- [27] X. Bonet-Monroig, R. Babbush, and T. E. O'Brien, , 1 (2019), [arXiv:1908.05628](#) .
- [28] H. Y. Huang, R. Kueng, and J. Preskill, *Nature Physics* , 1 (2020), [arXiv:2002.08953](#) .
- [29] J. R. Garrison and T. Grover, *Phys. Rev. X* **8**, 21026 (2018).
- [30] E. Chertkov and B. K. Clark, *Phys. Rev. X* **8**, 31029 (2018).
- [31] M. Greiter, V. Schnells, and R. Thomale, *Physical Review B* **98**, 081113 (2018), [arXiv:1802.07827](#) .
- [32] A. Gheorghiu and M. J. Hoban, , 1 (2020), [arXiv:2002.12814](#) .
- [33] N. Karmarkar, in *Proceedings of the sixteenth annual ACM symposium on Theory of computing* (1984) pp. 302–311.
- [34] M. Grötschel, L. Lovász, and A. Schrijver, *Algorithms and Combinatorics* (1993).
- [35] J. E. Kelley, Jr, *Journal of the society for Industrial and Applied Mathematics* **8**, 703 (1960).
- [36] A. T. Kalai and S. Vempala, *Mathematics of Operations Research* **31**, 253 (2006).

- [37] Y. T. Lee, A. Sidford, and S. C.-W. Wong, in *2015 IEEE 56th Annual Symposium on Foundations of Computer Science*, Vol. 2015-Decem (IEEE, 2015) pp. 1049–1065, [arXiv:1508.04874](#) .
- [38] H. Jiang, Y. T. Lee, Z. Song, and S. C.-w. Wong, [arXiv \(2020\)](#), [arXiv:2004.04250](#) .
- [39] Y. T. Lee, A. Sidford, and S. S. Vempala, (2017), [arXiv:1706.07357](#) .
- [40] D. S. Abrams and S. Lloyd, *Phys. Rev. Lett.* **83**, 5162 (1999).
- [41] A. Peruzzo, J. McClean, P. Shadbolt, M.-H. Yung, X.-Q. Zhou, P. J. Love, A. Aspuru-Guzik, and J. L. O’Brien, *Nature Communications* **5**, 4213 (2014).
- [42] O. Higgott, D. Wang, and S. Brierley, *Quantum* **3**, 156 (2019).
- [43] J. R. McClean, J. Romero, R. Babbush, and A. Aspuru-Guzik, *New Journal of Physics* **18**, 023023 (2016).
- [44] K. M. Nakanishi, K. Mitarai, and K. Fujii, *Physical Review Research* **1**, 033062 (2019), [arXiv:1810.09434](#) .
- [45] T. Jones, S. Endo, S. McArdle, X. Yuan, and S. C. Benjamin, *Physical Review A* **99**, 062304 (2019).
- [46] A. Kandala, A. Mezzacapo, K. Temme, M. Takita, M. Brink, J. M. Chow, and J. M. Gambetta, *Nature* **549**, 242 (2017).
- [47] B. Commeau, M. Cerezo, Z. Holmes, L. Cincio, P. J. Coles, and A. Sornborger, , 1 (2020), [arXiv:2009.02559](#) .
- [48] A. W. ROBERTS and D. E. VARBERG, (1973).
- [49] K. Mitarai, M. Negoro, M. Kitagawa, and K. Fujii, *Physical Review A* **98**, 032309 (2018).
- [50] R. Sweke, F. Wilde, J. Meyer, M. Schuld, P. K. Fährmann, B. Meynard-Piganeau, and J. Eisert, , 1 (2019), [arXiv:1910.01155](#) .
- [51] A. Arrasmith, L. Cincio, R. D. Somma, and P. J. Coles, , 1 (2020), [arXiv:2004.06252](#) .
- [52] R. Islam, R. Ma, P. M. Preiss, M. E. Tai, A. Lukin, M. Rispoli, and M. Greiner, *Nature* **528**, 77 (2015).
- [53] X. Yuan, S. Endo, Q. Zhao, Y. Li, and S. C. Benjamin, *Quantum* **3**, 191 (2019).
- [54] J. Wu and T. H. Hsieh, *Physical review letters* **123**, 220502 (2019).
- [55] X. Xu, J. Sun, S. Endo, Y. Li, S. C. Benjamin, and X. Yuan, **2**, 1 (2019), [arXiv:1909.03898](#) .
- [56] Y. Wang, G. Li, and X. Wang, , 1 (2020), [arXiv:2005.08797](#) .
- [57] Y. Shingu, Y. Seki, S. Watabe, S. Endo, Y. Matsuzaki, S. Kawabata, T. Nikuni, and H. Hakoshima, , 1 (2020), [arXiv:2007.00876](#) .
- [58] A. Valenti, E. van Nieuwenburg, S. Huber, and E. Greplova, *Physical Review Research* **1**, 033092 (2019), [arXiv:1907.02540](#) .
- [59] M. A. Nielsen and I. Chuang, “Quantum computation and quantum information,” (2002).

Supplementary Material

Appendix A: Hamiltonian Learning Algorithm

This section presents the main result, the hybrid quantum-classical Hamiltonian learning algorithm (HQHL). As discussed in Sec. II, the main utility of HQHL is to solve the dual program:

$$\boldsymbol{\mu} = \arg \min_{\boldsymbol{\nu}} \log Z_{\beta}(\boldsymbol{\nu}) + \beta \sum_{\ell=1}^m \nu_{\ell} e_{\ell}. \quad (\text{A1})$$

with the partition function $Z_{\beta}(\boldsymbol{\nu}) := \text{Tr}(e^{-\beta \sum_{\ell=1}^m \nu_{\ell} E_{\ell}})$ and coefficients $\boldsymbol{\nu} := (\nu_1, \dots, \nu_m)$. Thus, the core of HQHL is to optimize the following objective function $L(\boldsymbol{\nu})$:

$$L(\boldsymbol{\nu}) := \log Z_{\beta}(\boldsymbol{\nu}) + \beta \sum_{\ell=1}^m \nu_{\ell} e_{\ell}. \quad (\text{A2})$$

In this paper, gradient-based methods are employed to do the optimization. Afterward, approximate interaction coefficients $\hat{\boldsymbol{\mu}}$ are obtained. In particular, a standard procedure for optimizing $L(\boldsymbol{\nu})$ is depicted in Fig. 5.

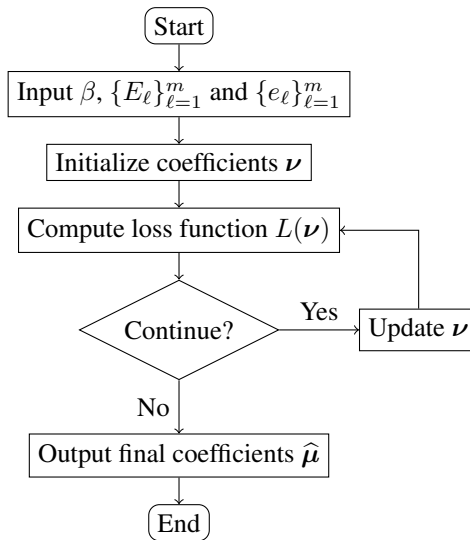


FIG. 5 Flowchart for Hamiltonian learning.

There are two important steps shown in Fig. 5: 1) Evaluation of objective function $L(\boldsymbol{\nu})$, 2) Update of coefficients $\boldsymbol{\nu}$. To provide practical methods for computing objective function and updating parameters, our HQHL algorithm sufficiently exploits the hybrid quantum-classical algorithms, which are compatible with NISQ devices. In the following, we introduce the main components of HQHL in detail. In particular, the procedures for computing the log-partition function $\log Z_{\beta}(\boldsymbol{\nu})$ in Sec. A 1.

1. Log-partition function estimation

Although there are many quantum and classical algorithms for partition function in the literature [18–22], these algorithms are either too expensive to implement or require complex quantum subroutines unavailable in the NISQ era. Thus, the existing algorithms are not suitable for our purpose. To find a practical

method implementable on NISQ devices, we propose to estimate the log-partition function using the system's free energy. Motivating our approach is the free energy's natural property—the global minimum of free energy is proportional to the corresponding log-partition function.

In the Hamiltonian learning setting, assuming the current parameters are $\boldsymbol{\nu}$, the system is then described by a parameterized Hamiltonian $H(\boldsymbol{\nu}) := \sum_{\ell=1}^m \nu_{\ell} E_{\ell}$. The free energy $F(\rho)$ is determined by the system's state ρ and inverse temperature β . Specifically, it is given by $F(\rho) := \text{Tr}(H(\boldsymbol{\nu})\rho) - \beta S(\rho)$. The log-partition function's property states the following relation:

$$\log Z_{\beta}(\boldsymbol{\nu}) = -\beta \min_{\rho} F(\rho). \quad (\text{A3})$$

The relation in Eq. (A3) implies that the log-partition function can be computed via solving an optimization program. However, this optimization requires an estimate of von Neumann entropy, and no efficient method for entropy estimation on shallow depth quantum circuits is known [32]. To overcome this challenge, we choose an alternate version of free energy $F(\rho)$ as the objective function, that is,

$$\log Z_{\beta}(\boldsymbol{\nu}) = -\beta \min_{\mathbf{p}} \left(\sum_{j=1}^N p_j \cdot \lambda_j + \beta^{-1} \sum_{j=1}^N p_j \log p_j \right), \quad (\text{A4})$$

where $\boldsymbol{\lambda} = (\lambda_1, \dots, \lambda_N)$ denotes the vector of eigenvalues of $H(\boldsymbol{\nu})$, $\mathbf{p} = (p_1, \dots, p_N)$ represents a probability distribution, and $N = 2^n$ is the dimension of the system. Besides, the proofs for Eqs. (A3), (A4) are quite common and provided in Sec. B 1.

To solve the optimization program in Eq. (A4), choose the objective function $C(\mathbf{p})$ as follows:

$$C(\mathbf{p}) := \sum_{j=1}^N p_j \cdot \lambda_j + \beta^{-1} \sum_{j=1}^N p_j \log p_j. \quad (\text{A5})$$

The part $\beta^{-1} \sum_{j=1}^N p_j \log p_j$ can be computed directly as the probability \mathbf{p} is stored on classical computers. Regarding the part $\sum_{j=1}^N p_j \cdot \lambda_j$, the eigenvalues $\boldsymbol{\lambda}$ of $H(\boldsymbol{\nu})$ are not known yet. To obtain eigenvalues, we call the subroutine SVQE, which will be introduced in Sec. A 1 a. It is worth pointing out that the SVQE algorithm cannot return all eigenvalues at once. Thus we can only access eigenvalues by the query. To be more specific, when we query SVQE with an integer j ($1 \leq j \leq N$), SVQE returns an estimate for eigenvalue λ_j . Furthermore, notice that value $\sum_{j=1}^N p_j \cdot \lambda_j$ can be regarded as an expectation, then we can use a sample mean of eigenvalues to approximate it. Combining these two parts, we can compute the log-partition function. Ultimately, we show the procedure in Fig. 6.

The method we present in Fig. 6 can effectively estimate $C(\mathbf{p})$ up to any precision with high probability. In particular, the probability can be improved to $1 - \eta$ by repeating the sampling procedure $O(\log(1/\eta))$ times and taking the median. The overall sample complexity of this method is shown below.

Proposition 1 *For any parameterized Hamiltonian $H(\boldsymbol{\nu}) = \sum_{\ell=1}^m \nu_{\ell} E_{\ell}$ with $E_{\ell} \in \{X, Y, Z, I\}^{\otimes n}$ and $\boldsymbol{\nu} \in \mathbb{R}^m$ and constant $\beta > 0$, suppose we are given access to a parameterized quantum circuit $U(\boldsymbol{\theta})$ that can learn $H(\boldsymbol{\nu})$'s eigenvectors, then the objective function $C(\mathbf{p})$ can be computed up to precision ϵ with probability larger than $2/3$ by taking $T = O(m \|\boldsymbol{\nu}\|_2^2 / \epsilon^2)$ samples. Furthermore, the probability can be improved to $1 - \eta$ costing an additional multiplicative factor of $O(\log(1/\eta))$.*

The proof can be found in Sec. B 2.

It is easy to see that estimation errors in Fig. 6 come from the termination condition and SVQE's outputs. Usually, the errors produced by the termination condition can be suppressed to arbitrarily small by allowing sufficiently many iterations. Thus we focus on analyzing the errors produced by SVQE in the following.

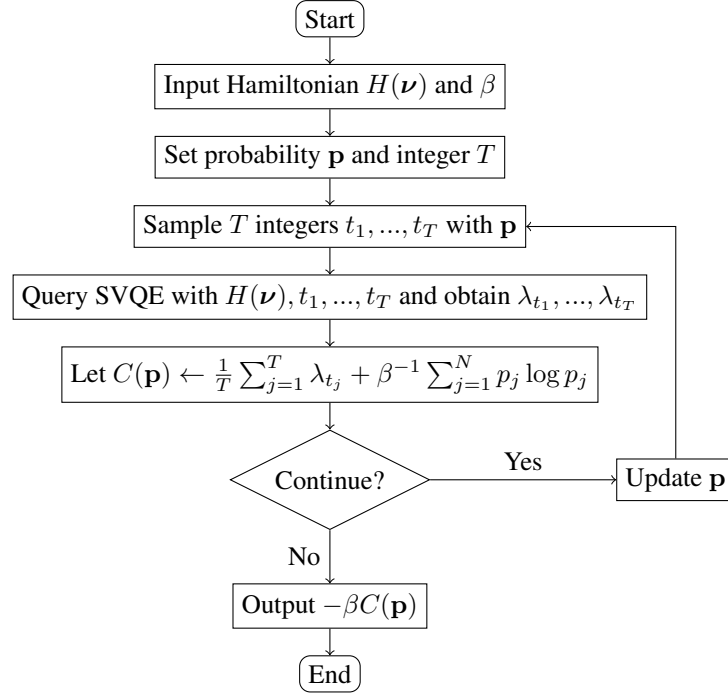


FIG. 6 Flowchart for estimating log-partition function. For simplicity, we here omit taking the median.

Lemma 1 Let $\hat{\lambda} = (\hat{\lambda}_1, \dots, \hat{\lambda}_N)$ denote the estimated eigenvalues from SVQE and define a function $G(\mathbf{p})$ as follows:

$$G(\mathbf{p}) := \sum_{j=1}^N p_j \hat{\lambda}_j + \beta^{-1} \sum_{j=1}^N p_j \log p_j. \quad (\text{A6})$$

Let $\hat{\mathbf{p}}^*$ be the global optimal point of $G(\mathbf{p})$, that is, for any probability distribution \mathbf{p} , we have $G(\hat{\mathbf{p}}^*) \leq G(\mathbf{p})$. Meanwhile, suppose \mathbf{p}^* is the global optimal point of $C(\mathbf{p})$. Then, we have

$$|G(\hat{\mathbf{p}}^*) - C(\mathbf{p}^*)| \leq \|\hat{\lambda} - \lambda\|_{\infty}. \quad (\text{A7})$$

Proof Since functions $C(\mathbf{p})$ and $G(\mathbf{p})$ reach their global minimums at points \mathbf{p}^* and $\hat{\mathbf{p}}^*$ respectively, then we have

$$C(\hat{\mathbf{p}}^*) \geq C(\mathbf{p}^*), \quad (\text{A8})$$

$$G(\hat{\mathbf{p}}^*) \leq G(\mathbf{p}^*). \quad (\text{A9})$$

Besides, we also have another relation:

$$|C(\mathbf{p}) - G(\mathbf{p})| = \left| \sum_{j=1}^N p_j (\hat{\lambda}_j - \lambda_j) \right| \leq \|\hat{\lambda} - \lambda\|_{\infty}, \quad (\text{A10})$$

where $\|\cdot\|_{\infty}$ denotes the maximum norm.

Combining the above inequalities, we have the following result:

$$C(\mathbf{p}^*) \leq C(\hat{\mathbf{p}}^*) \leq G(\hat{\mathbf{p}}^*) + \|\hat{\lambda} - \lambda\|_{\infty} \leq G(\mathbf{p}^*) + \|\hat{\lambda} - \lambda\|_{\infty} \leq C(\mathbf{p}^*) + 2\|\hat{\lambda} - \lambda\|_{\infty}. \quad (\text{A11})$$

Then the inequality in Eq. (A7) is proved. \blacksquare

Recalling that the log-partition function $\log Z_{\beta}(\nu)$ is equal to $-\beta C(\mathbf{p}^*)$, Lemma 1 indicates that the log-partition function estimate's error is less than $\beta \|\hat{\lambda} - \lambda\|_{\infty}$. In other words, the accurate log-partition function estimates are guaranteed by accurate eigenvalues from SVQE.

a. Stochastic variational quantum eigensolver

Extracting the information about eigenvalues of a Hamiltonian is the major subroutine for log-partition function estimation. We therefore present the SVQE algorithm in this section. Explicitly, we first exploit eigenvalues' variational property to formulate the diagonalization task as an optimization program and then show a hybrid quantum-classical procedure to solve this program.

Recall that, for any Hermitian matrix, eigenvalues $\boldsymbol{\lambda}$ of matrix majorize its diagonal elements $\mathbf{d} = (d_1, \dots, d_N)$, i.e., $\boldsymbol{\lambda} \succ \mathbf{d}$. In the meanwhile, the dot function with increasingly ordered vector is a Schur concave function [48]. Along with these two facts, suppose we are given probability distribution $\mathbf{q} = (q_1, \dots, q_N)$ such that $q_1 < q_2 < \dots < q_N$, then we have

$$\boldsymbol{\lambda} \cdot \mathbf{q} \leq \mathbf{d} \cdot \mathbf{q}. \quad (\text{A12})$$

Particularly, the equality in Eq. (A12) holds when diagonal elements are eigenvalues. It indicates an approach for computing eigenvalues is to find diagonal elements that satisfy the equality in Eq. (A12). To compute diagonal elements d_j , we utilize a parameterized quantum circuit $U(\boldsymbol{\theta})$ and a computational basis $|\psi_j\rangle$ to generate a parameterized ansatz $U(\boldsymbol{\theta})|\psi_j\rangle$. Furthermore, let $d_j = \langle \psi_j | U^\dagger(\boldsymbol{\theta}) H(\boldsymbol{\nu}) U(\boldsymbol{\theta}) | \psi_j \rangle$. Using the inequality in Eq. (A12), we formulate the task as an optimization program. Specifically speaking, the task is optimizing a stochastic mean $M(\boldsymbol{\theta})$ of energies of the Hamiltonian $H(\boldsymbol{\nu})$, defined below:

$$M(\boldsymbol{\theta}) := \sum_{j=1}^N q_j \cdot \langle \psi_j | U^\dagger(\boldsymbol{\theta}) H(\boldsymbol{\nu}) U(\boldsymbol{\theta}) | \psi_j \rangle. \quad (\text{A13})$$

After the optimization program, the final diagonal elements $\{d_j\}_{j=1}^N$ are the estimates for eigenvalues $\boldsymbol{\lambda}$.

The solution procedure SVQE can be effectively implemented on NISQ devices as long as the objective function $M(\boldsymbol{\theta})$ can be efficiently computed. Next, we give a procedure for computing $M(\boldsymbol{\theta})$ and then analyze the sample complexity in the following theorem. Regarding computing $M(\boldsymbol{\theta})$, since there are exponentially many diagonal elements, we cannot directly compute all diagonal elements when the Hamiltonian has many qubits. Notice that $M(\boldsymbol{\theta})$ can be regarded as an expectation of the probability distribution \mathbf{q} . Thus, we can compute $M(\boldsymbol{\theta})$ by a sampling procedure. Specifically, the procedure proceeds by sampling indices k_1, \dots, k_T according to \mathbf{q} , and then computing energy $\langle \psi_{k_j} | U^\dagger(\boldsymbol{\theta}) H(\boldsymbol{\nu}) U(\boldsymbol{\theta}) | \psi_{k_j} \rangle$ for $j = 1, \dots, T$. Finally, the average of all energies $\langle \psi_{k_j} | U^\dagger(\boldsymbol{\theta}) H(\boldsymbol{\nu}) U(\boldsymbol{\theta}) | \psi_{k_j} \rangle$ is an estimate for $M(\boldsymbol{\theta})$. In particular, this procedure can compute the objective function $M(\boldsymbol{\theta})$ up to arbitrary precision with high probability. Ultimately, we present a diagram to illustrate SVQE in Fig. 7. Furthermore, by Chernoff bounds, the probability can be boosted to arbitrarily high probability $1 - \eta$, costing an extra multiplicative factor of $O(\log(1/\eta))$.

Proposition 2 Consider a parameterized Hamiltonian $H(\boldsymbol{\nu}) = \sum_{\ell=1}^m \nu_\ell E_\ell$ with Pauli operators $E_\ell \in \{X, Y, Z, I\}^{\otimes n}$ and constants $\nu_\ell \in [-1, 1]$. Given any constants $\epsilon > 0$, $\eta \in (0, 1)$, $\beta > 0$, the objective function $M(\boldsymbol{\theta})$ in SVQE can be estimated up to precision ϵ with probability at least $1 - \eta$, costing TD samples with $T = O(m \|\boldsymbol{\nu}\|_2^2 / \epsilon^2)$ and $D = O(\log(1/\eta))$. Besides, the total number of measurements is given below:

$$O\left(\frac{mTD \|\boldsymbol{\nu}\|_1^2 (n + \log(m/\eta))}{\epsilon^2}\right). \quad (\text{A14})$$

The proof can be found in Sec. B 3.

In HLP, each element of $\boldsymbol{\nu}$ is assumed to lie in the interval $[-1, 1]$. Hence, Proposition 2 implies that the sample complexity scales polynomially in the system's size. Overall, the above discussion implies that our hybrid quantum-classical method for log-partition function and Hamiltonian learning is practical on NISQ computers.

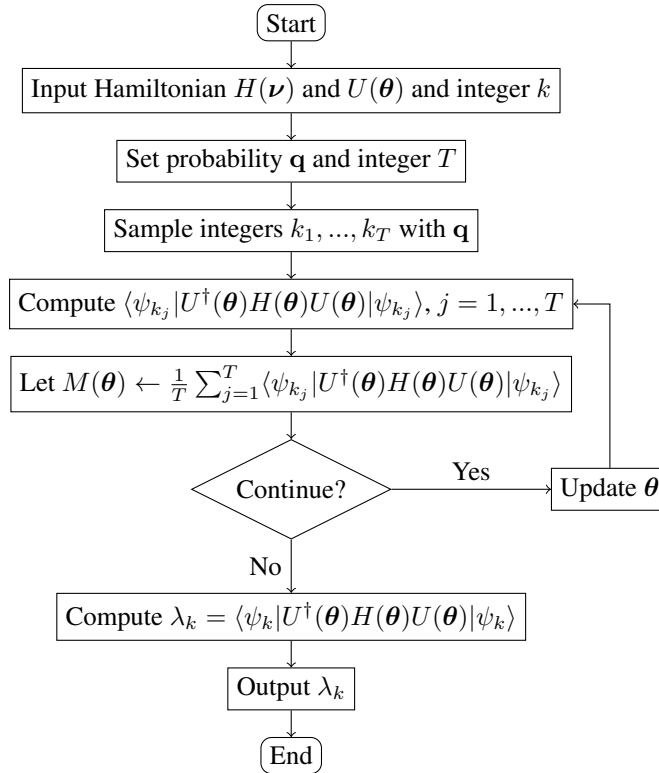


FIG. 7 Flowchart for stochastic variational quantum eigensolver. For simplicity, we here omit taking the median.

Appendix B: Supplementary proofs

1. Proofs for Eqs. (A3)-(A4)

Consider a Hamiltonian $H \in \mathbb{C}^{N \times N}$ and a constant $\beta > 0$, then the system's free energy is given by $F(\rho) = \text{Tr}(H\rho) - \beta^{-1}S(\rho)$. Recall the fact [59] that

$$S(\rho) \leq -\sum_{j=1}^N \rho_{jj} \log \rho_{jj}, \quad (\text{S1})$$

where ρ_{jj} are the diagonal elements of quantum state ρ . Using this fact, for any state ρ , we can find a lower bound on free energy in the sense that

$$F(\rho) \geq \text{Tr}(H\rho) + \beta^{-1} \sum_{j=1}^N \rho_{jj} \log \rho_{jj}. \quad (\text{S2})$$

On the other hand, let U be a unitary such that $H = U\Lambda U^\dagger$, where $\Lambda = \text{diag}(\lambda_1, \dots, \lambda_N)$ is a diagonal matrix. Let $\tilde{\rho} = \text{diag}(\rho_{11}, \dots, \rho_{NN})$ be the diagonal matrix consisting of ρ 's diagonal elements and let $\sigma = U^\dagger \tilde{\rho} U$. It is easy to verify that $\text{Tr}(H\rho) = \text{Tr}(\Lambda\sigma)$. Furthermore, taking this relation into Eq. (S2)'s right hand side, we can find that

$$F(\rho) \geq \text{Tr}(\Lambda\sigma) - \beta^{-1}S(\sigma). \quad (\text{S3})$$

Notice that Eq. (S3)'s right-hand side is equal to $F(\tilde{\rho})$, then we have

$$F(\rho) \geq F(\tilde{\rho}). \quad (\text{S4})$$

The inequality in Eq. (S4) shows that free energy's global optimum is commuting with the Hamiltonian H .

According to the above discussion, we can rewrite the optimization program of finding free energy's minimal value as follows

$$\min_{\rho} F(\rho) = \min_{\mathbf{p}} \left(\sum_{j=1}^N \lambda_j p_j + \beta^{-1} \sum_{j=1}^N p_j \log p_j \right), \quad (\text{S5})$$

where \mathbf{p} represents an arbitrary probability distribution. Eq. (S5)'s right-hand side can be solved using the Lagrange multiplier method, and the optimum is given below:

$$\mathbf{p}^* := \frac{1}{Z} (e^{-\beta\lambda_1}, \dots, e^{-\beta\lambda_N}), \quad (\text{S6})$$

with $Z := \sum_{j=1}^N e^{-\beta\lambda_j}$.

Finally, the equalities in Eqs. (A3)-(A4) can be proved by taking \mathbf{p}^* into Eq. (S5)'s right-hand side and computing the minimal value.

2. Proof for Proposition 1

Lemma S1 For any parameterized Hamiltonian $H(\boldsymbol{\nu}) = \sum_{\ell=1}^m \nu_{\ell} E_{\ell}$ with $E_{\ell} \in \{X, Y, Z, I\}^{\otimes n}$, we have

$$\| H(\boldsymbol{\nu}) \| \leq \sqrt{m} \cdot \| \boldsymbol{\nu} \|_2. \quad (\text{S7})$$

where $\| \cdot \|$ denotes the spectral norm and $\| \cdot \|_2$ is the ℓ_2 -norm.

Proof Let U be the unitary that diagonalizes the Hamiltonian $H(\boldsymbol{\nu})$, and then we can use the following form to represent $H(\boldsymbol{\nu})$.

$$H(\boldsymbol{\nu}) = \sum_{j=1}^N \lambda_j \cdot U |\psi_j\rangle \langle \psi_j| U^{\dagger}, \quad (\text{S8})$$

where $|\psi_1\rangle, \dots, |\psi_N\rangle$ are the computational basis.

Typically, each eigenvalue is represented as follows:

$$\lambda_j = \langle \psi_j | U^{\dagger} H(\boldsymbol{\nu}) U | \psi_j \rangle \quad (\text{S9})$$

$$= \sum_{\ell=1}^m \nu_{\ell} \langle \psi_j | U^{\dagger} E_{\ell} U | \psi_j \rangle \quad (\text{S10})$$

Then, applying the Cauchy-Schwarz inequality leads to an upper bound on each eigenvalue:

$$(\lambda_j)^2 \leq \sum_{\ell=1}^m (\nu_{\ell})^2 \cdot \sum_{\ell=1}^m (\langle \psi_j | U^{\dagger} E_{\ell} U | \psi_j \rangle)^2. \quad (\text{S11})$$

Meanwhile, recalling that all E_{ℓ} are Pauli matrix tensor product, we can obtain an upper bound below:

$$(\lambda_j)^2 \leq m \sum_{\ell=1}^m (\nu_{\ell})^2. \quad (\text{S12})$$

Ranging j in $\{1, \dots, N\}$ in Eq. (S12), the maximal eigenvalue is upper bounded by $\sqrt{m} \|\boldsymbol{\nu}\|_2$, validating the claim. \blacksquare

Proposition 1 For any parameterized Hamiltonian $H(\boldsymbol{\nu}) = \sum_{\ell=1}^m \nu_\ell E_\ell$ with $E_\ell \in \{X, Y, Z, I\}^{\otimes n}$ and $\boldsymbol{\nu} \in \mathbb{R}^m$ and constant $\beta > 0$, suppose we are given access to a parameterized quantum circuit $U(\boldsymbol{\theta})$ that can learn $H(\boldsymbol{\nu})$'s eigenvectors, then the objective function $C(\mathbf{p})$ can be computed up to precision ϵ with probability larger than $2/3$ by taking $T = O(m\|\boldsymbol{\nu}\|_2^2/\epsilon^2)$ samples. Furthermore, the probability can be improved to $1 - \eta$ costing an additional multiplicative factor of $O(\log(1/\eta))$.

Proof Since the expression $\sum_{j=1}^N p_j \lambda_j$ is regarded as an expectation, then we can estimate it by the sample mean with high accuracy and probability. To be specific, let X denote a random variable that takes value λ_j with probability p_j . Then, this expression can be written as

$$\mathbf{E}[X] = \sum_{j=1}^N p_j \lambda_j. \quad (\text{S13})$$

Furthermore, recall Chebyshev's inequality, then we have

$$\Pr(|\bar{X} - \mathbf{E}[X]| \leq \epsilon) \geq 1 - \frac{\mathbf{Var}[X]}{T\epsilon^2}. \quad (\text{S14})$$

where $\bar{X} = \frac{1}{T}(X_1 + X_2 + \dots + X_T)$ and $\mathbf{Var}[X]$ is the variance of X . Technically, we can set large T to increase the probability. Here, we only need to choose T such that

$$\frac{\mathbf{Var}[X]}{T\epsilon^2} = \frac{2}{3}. \quad (\text{S15})$$

Note that the second moment $\mathbf{E}[X^2]$ bounds the variance $\mathbf{Var}[X]$. Meanwhile, the second moment of X is bounded by the squared spectral norm of H , shown below.

$$\mathbf{E}[X^2] = \sum_{j=1}^N p_j (\lambda_j)^2 \quad (\text{S16})$$

$$\leq \sum_{j=1}^N p_j \|H(\boldsymbol{\nu})\|^2 \quad (\text{S17})$$

$$= \|H(\boldsymbol{\nu})\|^2. \quad (\text{S18})$$

The inequality is due to the fact that each eigenvalue is less than the spectral norm. Apply Lemma S1, then we will obtain a bound on T :

$$T = \frac{3\mathbf{Var}[X]}{2\epsilon^2} \leq \frac{3\mathbf{E}[X^2]}{2\epsilon^2} \leq \frac{3m\|\boldsymbol{\nu}\|_2^2}{2\epsilon^2}. \quad (\text{S19})$$

Lastly, according to the Chernoff bound, we can boost the probability to $1 - \eta$ for any $\eta > 0$ by repeatedly computing the sample mean $O(\log(1/\eta))$ times and taking the median of all sample means. ■

3. Proof for Proposition 2

Lemma S2 Consider a parameterized Hamiltonian $H(\boldsymbol{\nu}) = \sum_{\ell=1}^m \nu_\ell E_\ell$ with $E_\ell \in \{X, Y, Z, I\}^{\otimes n}$. For any unitary U and state $|\psi\rangle$, estimating the value $\langle \psi | U^\dagger H(\boldsymbol{\nu}) U | \psi \rangle$ up to precision ϵ with probability at least $1 - \eta$ requires a sample complexity of

$$O\left(\frac{m\|\boldsymbol{\nu}\|_1^2 \log(m/\eta)}{\epsilon^2}\right). \quad (\text{S20})$$

Proof First, we rewrite the value $\langle \psi | U^\dagger H(\boldsymbol{\nu}) U | \psi \rangle$ as follows:

$$\langle \psi | U^\dagger H(\boldsymbol{\nu}) U | \psi \rangle = \sum_{\ell=1}^m \nu_\ell \langle \psi | U^\dagger E_\ell U | \psi \rangle. \quad (\text{S21})$$

Second, we count the required number of measurements to estimate the value $\langle \psi | U^\dagger E_\ell U | \psi \rangle$ up to precision $\epsilon / \|\boldsymbol{\nu}\|_1$ with probability at least $1 - \eta/m$, where $\|\cdot\|_1$ denotes the ℓ_1 -norm. Since the Pauli operator, E_ℓ , has eigenvalues ± 1 , we can partition E_ℓ 's eigenvectors into two sets, corresponding to positive and negative eigenvalues, respectively. For convenience, we call the measurement outcome corresponding to eigenvalue 1 as the positive measurement outcome and the rest as the negative measurement outcome. We define a random variable X in the sense that

$$X = \begin{cases} 1, & \text{Pr [Positive measurement outcome]} \\ -1, & \text{Pr [Negative measurement outcome]} \end{cases} \quad (\text{S22})$$

It is easy to verify that $\mathbf{E}[X] = \langle \psi | U^\dagger E_\ell U | \psi \rangle$. Thus, an approach to compute value $\langle \psi | U^\dagger E_\ell U | \psi \rangle$ is computing an estimate for the expectation $\mathbf{E}[X]$. Meanwhile, consider that $\mathbf{E}[X^2] \leq 1$, then the required number of samples is $O(\|\boldsymbol{\nu}\|_1^2 \log(m/\eta) / \epsilon^2)$.

Lastly, for $\langle \psi | U^\dagger H(\boldsymbol{\nu}) U | \psi \rangle$, the estimate's maximal error is $\|\boldsymbol{\nu}\|_1 \cdot \epsilon / \|\boldsymbol{\nu}\|_1 = \epsilon$. By union bound, the overall failure probability is less than $m \cdot \eta/m = \eta$. Thus, the claim is proved. \blacksquare

Proposition 2 Consider a parameterized Hamiltonian $H(\boldsymbol{\nu}) = \sum_{\ell=1}^m \nu_\ell E_\ell$ with Pauli operators $E_\ell \in \{X, Y, Z, I\}^{\otimes n}$ and constants $\nu_\ell \in [-1, 1]$. Given any constants $\epsilon > 0$, $\eta \in (0, 1)$, $\beta > 0$, the objective function $M(\boldsymbol{\theta})$ in SVQE can be estimated up to precision ϵ with probability at least $1 - \eta$, costing TD samples with $T = O(m\|\boldsymbol{\nu}\|_2^2/\epsilon^2)$ and $D = O(\log(1/\eta))$. Besides, the total number of measurements is given below:

$$O\left(\frac{mTD\|\boldsymbol{\nu}\|_1^2(n + \log(m/\eta))}{\epsilon^2}\right). \quad (\text{S23})$$

Proof Let Y denote a random variable that takes value $\langle \psi_j | U^\dagger(\boldsymbol{\theta}) H(\boldsymbol{\nu}) U(\boldsymbol{\theta}) | \psi_j \rangle$ with probability q_j , then the objective function $M(\boldsymbol{\theta})$ can be rewritten as

$$\mathbf{E}[Y] = M(\boldsymbol{\theta}). \quad (\text{S24})$$

By Chebyshev's inequality, the expectation can be computed by taking enough samples of Y and averaging them. Note that the variance of Y determines the number of samples, and the absolute value Y is less than the spectral norm $\|H(\boldsymbol{\nu})\|$, i.e., $|Y| \leq \|H(\boldsymbol{\nu})\|$. Along with Lemma S1, it is easy to see that the required number of Y 's samples for obtaining an estimate with error $\epsilon/2$ and probability larger than $2/3$ is $T = O(m\|\boldsymbol{\nu}\|_2^2/\epsilon^2)$. Furthermore, by Chernoff bounds, the probability can be improved to $1 - \eta/2$ at an additional cost of multiplicative factor of $D = O(\log(1/\eta))$.

On the other hand, each sample Y 's value has to be determined by performing the measurement. Since $|\psi_j\rangle$ is a computational basis, hence Y can take at most 2^n different values. To ensure the probability for estimating $\mathbf{E}[Y]$ larger than $1 - \eta$, the probability of each estimate $\langle \psi_j | U^\dagger(\boldsymbol{\theta}) H(\boldsymbol{\nu}) U(\boldsymbol{\theta}) | \psi_j \rangle$ only needs to be at least $1 - \eta/2^{n+1}$. By union bound, the overall failure probability is at most $\eta/2 + \eta \cdot \frac{TD}{2^{n+1}} < \eta$ (For large Hamiltonians, the number of samples TD can be significantly less than dimension 2^n). Besides, according to Lemma S2, $\langle \psi_j | U^\dagger(\boldsymbol{\theta}) H(\boldsymbol{\nu}) U(\boldsymbol{\theta}) | \psi_j \rangle$'s estimate within accuracy $\epsilon/2$ and probability $1 - \eta/2^{n+1}$ requires a sample complexity of $O(m\|\boldsymbol{\nu}\|_1^2(n + \log(m/\eta))/\epsilon^2)$. Thus, the overall number of measurements is the product of the number of samples $TD = O(m\|\boldsymbol{\nu}\|_2^2 \log(1/\eta)/\epsilon^2)$ and each sample's sample complexity

$O(m\|\boldsymbol{\nu}\|_1^2(n + \log(m/\eta))/\epsilon^2)$. In other words, the objective function $M(\boldsymbol{\theta})$'s estimate within error ϵ and probability $1 - \eta$ requires a sample complexity of

$$O\left(TD \cdot \frac{m\|\boldsymbol{\nu}\|_1^2(n + \log(m/\eta))}{\epsilon^2}\right) = O\left(\frac{m^2\|\boldsymbol{\nu}\|_1^2\|\boldsymbol{\nu}\|_2^2 \log(1/\eta)(n + \log(m/\eta))}{\epsilon^4}\right).$$

■

4. Proof for Proposition 3

Proposition 3 (Correctness) Consider a parameterized Hamiltonian $H(\boldsymbol{\nu})$ and its Gibbs state $\rho_\beta(\boldsymbol{\nu})$. Suppose the $U(\boldsymbol{\theta})$ from SVQE (cf. Algorithm 3) and $\widehat{\mathbf{p}}^*$ from log-partition function estimation procedure (cf. Algorithm 2) are optimal. Define a density operator ρ_β^* as follows:

$$\rho_\beta^* := \sum_{j=1}^N \widehat{p}_j^* \cdot U(\boldsymbol{\theta}) |\psi_j\rangle\langle\psi_j| U^\dagger(\boldsymbol{\theta}). \quad (\text{S25})$$

where $\{|\psi_j\rangle\}$ denote the computational basis. Denote the estimated eigenvalues by $\widehat{\boldsymbol{\lambda}}$, where $\widehat{\lambda}_j = \langle\psi_j|U^\dagger(\boldsymbol{\theta})H(\boldsymbol{\nu})U(\boldsymbol{\theta})|\psi_j\rangle$. Then, ρ_β^* is an approximate of $\rho_\beta(\boldsymbol{\nu})$ in the sense that

$$D(\rho_\beta^*, \rho_\beta(\boldsymbol{\nu})) \leq \sqrt{2\beta \|\widehat{\boldsymbol{\lambda}} - \boldsymbol{\lambda}\|_\infty}. \quad (\text{S26})$$

where $D(\cdot, \cdot)$ denotes the trace distance, $\boldsymbol{\lambda}$ represent $H(\boldsymbol{\nu})$'s true eigenvalues.

Proof Recalling the expressions of $C(\mathbf{p}^*)$ and $G(\widehat{\mathbf{p}}^*)$ in Eqs. (A5), (A6), it is easy to verify the following inequalities:

$$F(\rho_\beta(\boldsymbol{\nu})) = C(\mathbf{p}^*), \quad (\text{S27})$$

$$F(\rho_\beta^*) = G(\widehat{\mathbf{p}}^*). \quad (\text{S28})$$

where F denotes the free energy, i.e., $F(\rho) = \text{Tr}(H\rho) - \beta^{-1}S(\rho)$.

Using the result in Lemma 1, we will obtain the following inequality.

$$|F(\rho_\beta^*) - F(\rho_\beta(\boldsymbol{\nu}))| = |G(\widehat{\mathbf{p}}^*) - C(\mathbf{p}^*)| \leq \|\widehat{\boldsymbol{\lambda}} - \boldsymbol{\lambda}\|_\infty. \quad (\text{S29})$$

In the meanwhile, a property of the free energy says that

$$F(\rho_\beta^*) = F(\rho_\beta(\boldsymbol{\nu})) + \beta^{-1}S(\rho_\beta^*||\rho_\beta(\boldsymbol{\nu})). \quad (\text{S30})$$

where $S(\rho_\beta^*||\rho_\beta(\boldsymbol{\nu}))$ is the relative entropy. Rewriting the above equation as follows:

$$F(\rho_\beta^*) - F(\rho_\beta(\boldsymbol{\nu})) = \beta^{-1}S(\rho_\beta^*||\rho_\beta(\boldsymbol{\nu})). \quad (\text{S31})$$

Combining the relations in Eqs. (S29) and (S31), we obtain the following inequality:

$$S(\rho_\beta^*||\rho_\beta(\boldsymbol{\nu})) \leq \beta \|\widehat{\boldsymbol{\lambda}} - \boldsymbol{\lambda}\|_\infty. \quad (\text{S32})$$

Lastly, according to Pinsker's inequality, the above inequality immediately leads to a bound on the trace distance between ρ_β and ρ_β^* in the sense that

$$D(\rho_\beta^*, \rho_\beta(\boldsymbol{\nu})) \leq \sqrt{2S(\rho_\beta^*||\rho_\beta(\boldsymbol{\nu}))} \leq \sqrt{2\beta \|\widehat{\boldsymbol{\lambda}} - \boldsymbol{\lambda}\|_\infty}. \quad (\text{S33})$$

The the claimed is proved. ■

5. Proof for Proposition 4

Proposition 4 (Sample complexity) *Given $\epsilon > 0$ and $\eta \in (0, 1)$, Algorithm 4 can compute an estimate for the gradient $\nabla L(\boldsymbol{\nu})$ up to precision ϵ with probability larger than $1 - \eta$. Particularly, the overall number of samples is $KD = O(\beta^2 \log(m/\eta)/\epsilon^2)$ with $K = O(\beta^2/\epsilon^2)$ and $D = O(\log(2m/\eta))$. Besides, the total number of measurements is $O(KD \cdot m\beta^2(n + \log(m/\eta))/\epsilon^2)$.*

Proof Let Z_ℓ denote the random variable that takes value $\langle \psi_j | U^\dagger(\boldsymbol{\theta}) E_\ell U(\boldsymbol{\theta}) | \psi_j \rangle$ with probability \widehat{p}_j^* , for all $\ell = 1, \dots, m$. Then we have

$$\mathbf{E}[Z_\ell] = \sum_{j=1}^N \widehat{p}_j^* \cdot \langle \psi_j | U^\dagger(\boldsymbol{\theta}) E_\ell U(\boldsymbol{\theta}) | \psi_j \rangle. \quad (\text{S34})$$

Thus partial derivative can be computed in the following way

$$\frac{\partial L(\boldsymbol{\nu})}{\partial \nu_\ell} \approx -\beta \mathbf{E}[Z_\ell] + \beta e_\ell. \quad (\text{S35})$$

It implies that the estimate's error can be set as ϵ/β to ensure the gradient's maximal error less than ϵ .

Next, we determine the number of samples such that the overall failure probability for estimating the gradient is less than δ . Since the gradient has m partial derivatives, corresponding to $\mathbf{E}[Z_\ell]$, thus it suffices to estimate each with probability larger than $1 - \delta/m$. Meanwhile, each mean $\mathbf{E}[Z_\ell]$ can be computed by sampling. Notice that all $|Z_\ell| \leq 1$, by Chebyshev's inequality, then it suffices to take $K = O(\beta^2/\epsilon^2)$ samples to compute an estimate for each $\mathbf{E}[Z_\ell]$ with precision $\epsilon/2\beta$ and probability larger than $2/3$. Furthermore, by Chernoff bounds, the probability can be improved to $1 - \eta/2m$ at an additional cost of multiplicative factor of $D = O(\log(2m/\eta))$. It is worth pointing out that, for each variable Z_ℓ , the samples are taken according to the same probability distribution $\widehat{\mathbf{p}}^*$, thus it is natural to use the sampled states $|\psi_{t_j^s}\rangle$ (cf. Algorithm 4) to compute all means $\mathbf{E}[Z_\ell]$. Then the total number of samples is $KD = O(\beta^2 \log(m/\eta)/\epsilon^2)$.

On the other hand, each value $\langle \psi_j | U^\dagger(\boldsymbol{\theta}) E_\ell U(\boldsymbol{\theta}) | \psi_j \rangle$ in Eq. (S34) has to be computed by performing the measurement. Note that there are 2^n values $\langle \psi_j | U^\dagger(\boldsymbol{\theta}) E_\ell U(\boldsymbol{\theta}) | \psi_j \rangle$ in all. To ensure the mean estimate's failure probability less than $\eta/2m$, it suffices to suppress each value's failure probability to $\eta/2^{n+1}m$. Following the same discussion in Lemma S2, the estimate for value $\langle \psi_j | U^\dagger(\boldsymbol{\theta}) E_\ell U(\boldsymbol{\theta}) | \psi_j \rangle$ can be computed up to precision $\epsilon/2\beta$ using $O(\beta^2 \log(2^{n+1}m/\eta)/\epsilon^2)$ measurements.

Regarding the failure probability, by union bound, the overall failure probability is at most $m \cdot (\eta/2m + KD \cdot \eta/2^{n+1}m)$, where KD is the number of samples $KD = O(\beta^2 \log(m/\eta)/\epsilon^2)$. Especially, for larger Hamiltonians, the number of measurements is usually less than the dimension 2^n . Thus, the overall failure probability is less than η .

Lastly, the total number of measurements is given below:

$$m \cdot KD \cdot O(\beta^2 \log(2^{n+1}m/\eta)/\epsilon^2) = O(m\beta^4 \log(m/\eta) \log(2^{n+1}m/\eta)/\epsilon^4). \quad (\text{S36})$$

■